J. Phys. Chem. A **2006,** *110,* 1845−1849

Noble Gas−Transition-Metal Complexes: Coordination of VO_2 and VO_4 by Ar and Xe Atoms in Solid Noble Gas Matrixes

Yanying Zhao, Yu Gong, Mohua Chen, and Mingfei Zhou*

Department of Chemistry & Laser Chemistry Institute, Shanghai Key Laboratory of Molecular Catalysts and Innovative Materials, Fudan University, Shanghai 200433, People's Republic of China

Received: November 9, 2005; In Final Form: December 7, 2005

The matrix isolation infrared spectroscopic and quantum chemical calculation results indicate that vanadium oxides, VO_2 and VO_4, coordinate noble gas atoms in forming noble gas complexes. The results showed that VO_2 coordinates two Ar or Xe atoms and that VO_4 coordinates one Ar or Xe atom in solid noble gas matrixes. Hence, the VO_2 and VO_4 molecules trapped in solid noble gas matrixes should be regarded as the $VO_2(Ng)_2$ and $VO_4(Ng)$ (Ng = Ar or Xe) complexes. The total V−Ng binding energies were predicted to be 12.8, 18.2, 5.0, and 7.3 kcal/mol, respectively, for the $VO_2(Ar)_2$, $VO_2(Xe)_2$, $VO_4(Ar)$, and $VO_4(Xe)$ complexes at the CCSD(T)//B3LYP level of theory.

Introduction

The electronic and geometric structures of transition-metal oxides are of interest for the understanding of the catalytic properties of metal oxides. Particularly, vanadium oxide catalysts are widely used in the chemical industry and synthesis laboratories. The VO diatomic has been well studied both experimentally and theoretically.[1−8] Its ground state as well as several excited states was investigated in the gas phase. Studies have also been carried out for the higher oxide VO_x molecules.[9−16] The electronic structure information of the isolated VO_x ($x = 1-4$) species has been probed in the gas phase.[9,10] The matrix isolation technique played an important role in providing valuable spectral and structural properties of neutral vanadium oxide molecules. A superoxovanadium VO_4 species was suggested to be observed in photo-oxidation of $V(CO)_6$ in low-temperature matrixes containing O_2.[11] The VO, VO_2, VO_3, and VO_4 molecules in solid neon or argon matrixes have been produced by pulsed laser ablation generation method and have been characterized by electron spin resonance and infrared absorption spectroscopies.[12,13]

It is generally assumed that the oxide molecules trapped in solid neon or argon matrixes can be regarded as isolated "gas-phase" molecules.[17] Matrix shifts for most of covalently bonded molecules trapped in solid neon or argon often are quite small. However, considerable variations in the values of measured vibrational fundamentals in different noble gas matrixes have been observed for some metal oxide species.[18−21] The combined experimental and theoretical studies showed that actinide metal oxides such as CUO, UO_2, and UO_2^+ trapped in noble gas matrixes are coordinated by multiple noble gas atoms.[18−21] The CUO, UO_2, and UO_2^+ species trapped in solid noble gas matrixes should be regarded as the $CUO(Ng)_n$, $UO_2(Ng)_n$, and $[UO_2(Ng)_n]^+$ complexes, instead of isolated oxide molecules. Recent investigations in our laboratory also showed that transition-metal oxide cations, such as ScO^+ and YO^+, also form a variety of noble gas complexes in solid noble gas matrixes.[22,23] In this paper, we report that neutral transition-metal oxides, VO_2 and VO_4 are coordinated by noble gas atoms in forming the distinct transition metal− noble gas complexes.

Experimental and Computational Methods

The experimental setup for pulsed laser-ablation and matrix isolation Fourier transform infrared (FTIR) spectroscopic investigation has been described in detail previously.[24] Briefly, the 1064-nm fundamental of a Nd:YAG laser (20-Hz repetition rate and 8-ns pulse width) was focused onto a rotating metal vanadium target (Johnson Matthey, 99.9%) through a hole in a CsI window cooled normally to 12 K by means of a closed-cycle helium refrigerator. The laser-evaporated vanadium atoms were codeposited with oxygen and noble gas mixtures onto the CsI window. In general, matrix samples were deposited for 1−2 h at a rate of 3−5 mmol/h. The O_2/Xe/Ar mixtures were prepared in a stainless steel vacuum line using standard manometric technique. Isotopic $^{18}O_2$ (ISOTEC, 99%) was used without further purification. The infrared absorption spectra of the resulting sample were recorded on a Bruker IFS 113V spectrometer at 0.5-cm^{-1} resolution between 4000 and 400 cm^{-1} using a DTGS detector. After the infrared spectrum of the initial deposition had been recorded, the samples were warmed to the desired temperature, quickly recooled, and the spectrum taken, followed by repetition of these steps using higher temperatures.

Quantum chemical calculations were performed using the Gaussian 03 program.[25] The three-parameter hybrid functional according to Becke with additional correlation corrections due to Lee, Yang, and Parr (B3LYP)[26,27] and the second-order Møller−Plesset perturbation (MP2)[28] methods were utilized. The 6-311+G* basis set was used for O, V, and Ar atoms, and the SDD pseudopotential and basis set was used for Xe atom.[29,30] The geometries were fully optimized at both levels of theory. In addition, the single point energies of the structures optimized at the B3LYP level of theory were calculated using the CCSD(T) method with the same basis sets.[31] The harmonic vibrational frequencies were calculated at the B3LYP level, and zero-point vibrational energies (ZPVE) were derived.

Results and Discussion

Infrared Spectra. The reaction of laser-ablated vanadium atoms with oxygen in solid argon has been investigated

---

* To whom correspondence should be addressed. E-mail: mfzhou@fudan.edu.cn.

10.1021/jp056476s CCC: $33.50

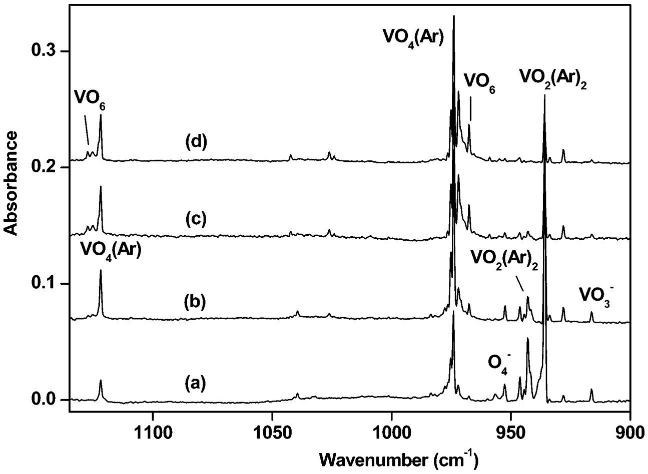

Figure 1. Infrared spectra in the 1140−900-cm^{-1} region from co-deposition of laser-ablated vanadium atoms with 1% O_2 in argon: (a) 1 h of sample deposition at 12 K, (b) after annealing to 35 K, (c) after annealing to 40 K, and (d) after annealing to 45 K.

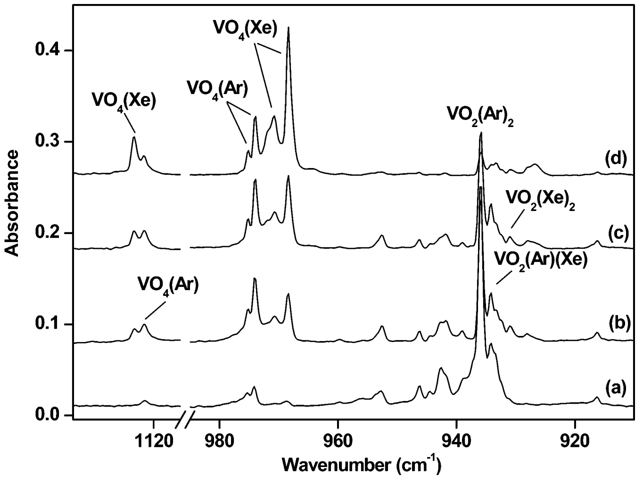

Figure 2. Infrared spectra in the 1135−1115- and 985−910-cm^{-1} regions from co-deposition of laser-ablated vanadium atoms with 1% O_2 + 1% Xe in argon: (a) 1 h of sample deposition at 12 K, (b) after annealing to 35 K, (c) after annealing to 40 K, and (d) after annealing to 45 K.

TABLE 1: Infrared Absorptions (cm^{-1}) from Co-Deposition of Laser-Ablated V Atoms with Oxygen/Xenon Mixtures in Excess Argon

$^{16}O_2$	$^{18}O_2$	assignment	
1127.2	1061.7	VO_6	O−O stretch
1121.9	1055.3	VO_4(Ar)	O−O stretch
1123.8	1060.9	VO_4(Xe)	O−O stretch
975.3	932.0	VO_4(Ar)	sym-OVO stretch
974.1	936.7	VO_4(Ar)	asym-OVO stretch
971.9	934.7	VO_4(Ar)	site
970.9	927.6	VO_4(Xe)	sym-OVO stretch
968.4	931.3	VO_4(Xe)	asym-OVO stretch
967.6	930.5	VO_6	asym-OVO stretch
946.3	902.1	$VO_2(Ar)_2$	sym-OVO stretch
935.9	899.9	$VO_2(Ar)_2$	asym-OVO stretch
934.2	897.7	VO_2(Ar)(Xe)	asym-OVO stretch
931.0	895.4	$VO_2(Xe)_2$	asym-OVO stretch
555.6	533.4	VO_4(Ar)	V−O_2 stretch

previously,[13] and the vanadium oxide products have been identified from the effects of isotopic substitution in their infrared spectra and theoretical calculations. We first repeated the experiment of laser-ablated vanadium and oxygen reaction. The spectra in the 1140−900-cm^{-1} region from co-deposition of laser-ablated vanadium with 1.0% O_2 in argon are shown in Figure 1. The infrared spectra in the V−O stretching frequency region are about the same as that previous reported.[13] Besides the known metal independent O_3, O_3^-, O_4^-, and O_4^+ species,[32,33] absorptions at 1121.9, 975.3, 974.1, 946.3, 935.9, and 555.6 cm^{-1} were observed after 1 h of sample deposition at 12 K. The 946.3 and 935.9 cm^{-1} absorptions were previously assigned to the symmetric and antisymmetric V−O stretching vibrations of the bent VO_2 molecule.[13] The 1121.9-, 975.3-, 974.1-, and 555.6-cm^{-1} bands were attributed initially to the VO_4 molecule with a $OOVO_2$ (C_s) structure but have been reassigned later to VO_4 with a $(O_2)VO_2$ (C_{2v}) structure.[34] Weak absorptions due to VO_2^- (896.8 cm^{-1}) and VO_3^- (916.2 cm^{-1}) were also observed.[34] The VO_2 absorptions decreased on sample annealing; the VO_4 absorptions markedly increased on 35 K annealing (Figure 1, trace b) and slightly decreased on subsequent higher temperature annealing (Figure 1, traces c and d). New bands at 1125.4 and 967.6 cm^{-1} were produced on 35 K annealing and increased on higher temperature annealing.

Experiments were repeated by using oxygen doped with Xe in excess argon. Figure 2 shows the spectra in the 1135−1115- and 985−910-cm^{-1} regions from co-deposition of laser-ablated vanadium with 1.0% O_2 doped with 1.0% Xe in argon. The same product absorptions observed in the experiment without Xe doping were observed as described above. In addition, new absorptions at 1123.8, 970.9, 968.4, 934.2, and 931.0 cm^{-1} were produced on sample annealing to different temperatures (Figure 2, traces b−d). The 1123.8-, 970.9-, and 968.4-cm^{-1} bands increased markedly on annealing to higher temperatures and dominated the spectrum after sample annealing to 45 K (Figure 2, trace d). The product absorptions are listed in Table 1.

The experiments were repeated using the isotopic labeled $^{18}O_2$ doped with xenon in excess argon. The spectra in selected regions are shown in Figure 3. All the absorptions were shifted, and the band positions are listed in Table 1. A similar experiment was performed using a mixed 0.4% $^{16}O_2$ + 0.8% $^{16}O^{18}O$ + 0.4% $^{18}O_2$ + 1% Xe in argon sample, and the resulting spectra in the 1140−1040-cm^{-1} region are illustrated in Figure 4.

Calculation Results. Quantum chemical calculations were performed on the potential product molecules. The optimized structures at both the B3LYP and MP2 levels of theory are shown in Figure 5. The calculated vibrational frequencies are listed in Table 2. The calculated total V−Ng binding energies

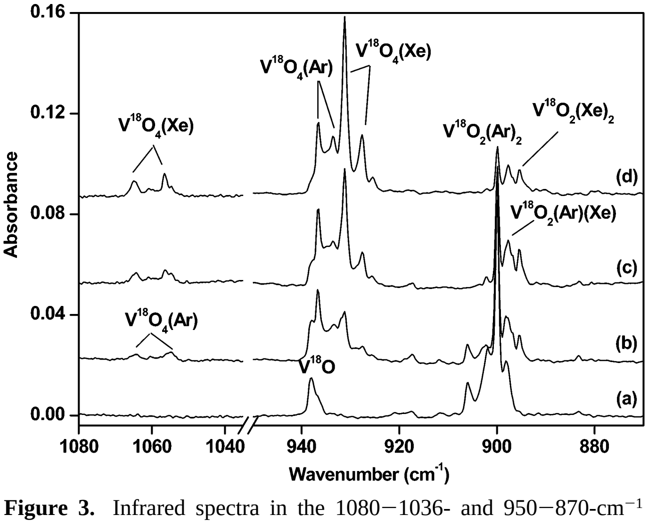

Figure 3. Infrared spectra in the 1080−1036- and 950−870-cm^{-1} regions from co-deposition of laser-ablated vanadium atoms with 1% $^{18}O_2$ + 1% Xe in argon: (a) 1 h of sample deposition at 12 K, (b) after annealing to 35 K, (c) after annealing to 40 K, and (d) after annealing to 45 K.

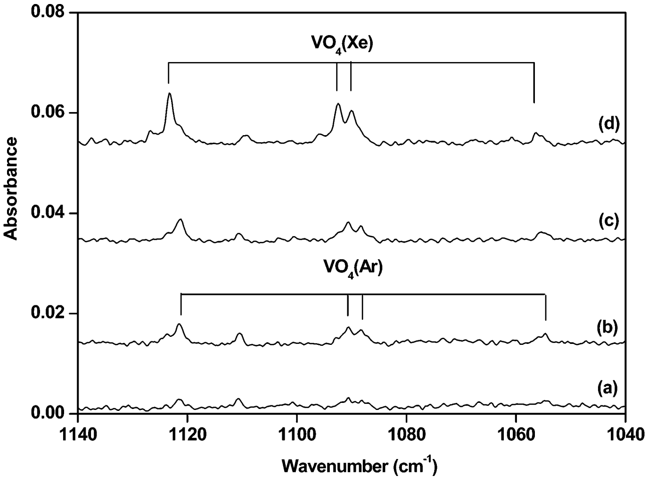

Figure 4. Infrared spectra in the 1140−1040-cm^{-1} region from co-deposition of laser-ablated vanadium atoms with 0.4% $^{16}O_2$ + 0.8% $^{16}O^{18}O$ + 0.4% $^{18}O_2$ + 1% Xe in argon: (a) 1 h of sample deposition at 12 K, (b) after annealing to 35 K, (c) after annealing to 40 K, and (d) after annealing to 45 K.

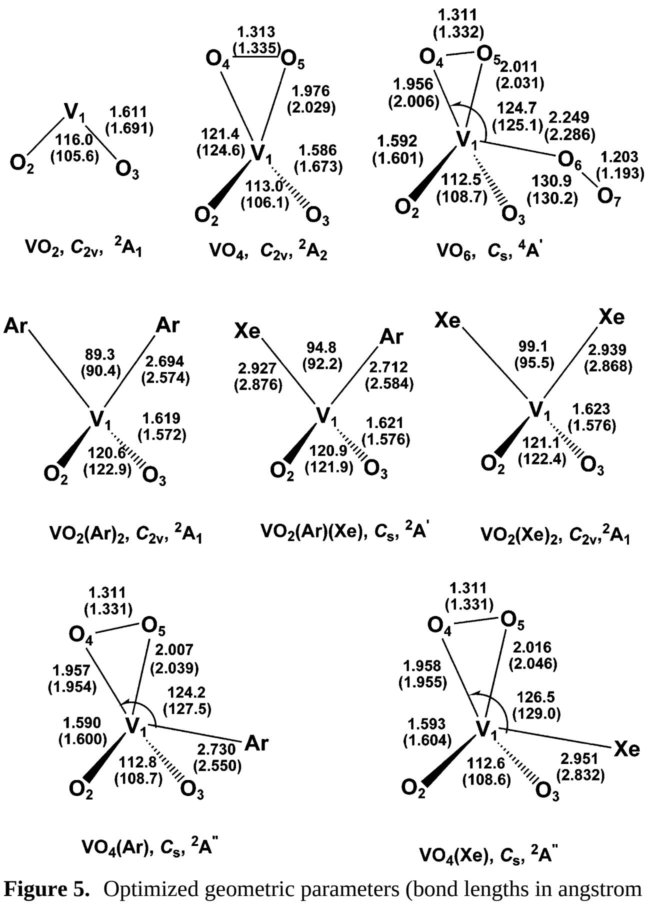

Figure 5. Optimized geometric parameters (bond lengths in angstrom and bond angles in degree) of the product species at the B3LYP and MP2 (values in parentheses) levels of theory.

and natural atomic charges are listed in Tables 3 and 4, respectively.

$VO_2(Ar)_{2-x}(Xe)_x$ (x = 0, 1, 2). The 946.3- and 935.9-cm^{-1} bands in solid argon were previously assigned to the symmetric and antisymmetric VO_2 stretching vibrations of VO_2 based on the observed isotopic shifts and splittings.[13] The symmetric stretching mode of VO_2 was determined to be 970 ± 40 cm^{-1} from anion photon electron spectroscopic study[9] and to be 993.0 cm^{-1} with electronic spectroscopy in the gas phase.[10] The large frequency difference between the gas phase and matrix values suggests that VO_2 may be coordinated by noble gas atoms in noble gas matrixes. To determine whether the VO_2 molecule trapped in solid matrixes is coordinated by noble gas atoms or not and to determine the number of noble gas atoms that bind intimately to VO_2 in the first coordination sphere, experiments were performed by using mixtures of argon doped with xenon. The spectra shown in Figure 2 demonstrate that two new absorptions at 934.2 and 931.0 cm^{-1} were produced when 1% xenon was doped into argon. The 934.2- and 931.0-cm^{-1} bands shifted to 897.7 and 895.4 cm^{-1} with $^{18}O_2$; the $^{16}O/^{18}O$ isotopic frequency ratios of 1.0407 and 1.0398 are characteristic of antisymmetric VO_2 stretching vibrations. These observations suggest that VO_2 coordinates two noble gas atoms in solid noble gas matrixes. Hence, the 946.3- and 935.9-cm^{-1} bands previously assigned to VO_2 in solid argon should be reassigned to the $VO_2(Ar)_2$ complex in solid argon, and the 934.2- and 931.0-cm^{-1} bands are due to the $VO_2(Ar)(Xe)$ and $VO_2(Xe)_2$ complexes in solid argon, resulting from the successive replacement of coordinated Ar atoms with Xe atoms. The symmetric VO_2 stretching modes for $VO_2(Ar)(Xe)$ and $VO_2(Xe)_2$ are too weak to be observed.

Quantum chemical calculations were performed to support the assignment, which indicated that VO_2 could coordinate two noble gas atoms. As shown in Figure 5, the VO_2 molecule and the $VO_2(Ar)_2$ and $VO_2(Xe)_2$ complexes were predicted to have a $^2A_1$ ground state with C_{2v} symmetry. Upon noble gas coordination, the V−O bond length elongated from 1.611 Å in VO_2 to 1.619 Å in $VO_2(Ar)_2$ and to 1.623 Å in $VO_2(Xe)_2$. The calculation results listed in Tables 2 and 3 also indicate that the total V−Ng binding energies increase monotonically with increasing Xe atom substitution, while the calculated VO_2 stretching frequencies of the $VO_2(Ar)_{2-x}(Xe)_x$ (x = 0,1,2) series exhibit the monotonic red-shift upon successively replacement of Ar atoms by Xe atoms. The calculated red-shifts of the antisymmetric VO_2 stretching mode for successively substituting Ar atoms by Xe atoms are 4.7 and 8.2 cm^{-1}, respectively, slightly larger than the experimentally determined shifts of 1.7 and 4.9 cm^{-1}.

Similar to the other previously characterized metal−noble gas complexes,[18−23] the bonding in the above-characterized $VO_2(Ng)_2$ complexes also involves the Lewis acid−base interactions, in which electron density in the Ng lone pairs is donated into vacant orbitals of the vanadium center. The VO_2 molecule has a $^2A_1$ ground state. The $11a_1$ LUMO is primarily a nonbonding hybrid of the V 4s and $3d_{z^2}$ orbitals that is directed away from the O atoms. The $4b_1$ LUMO+1 is a bonding π orbital composed of the V 3d orbital and the O 2p orbitals. These orbitals are the primary acceptor orbitals for donation from the noble gas atoms. Consistent with the above notions, the calculated natural atomic charges for the metal center listed in Table 4 decrease upon coordination of noble gas atoms and upon successively replacement of argon atoms by xenon atoms. The natural atomic charges on vanadium drop from +1.36 in VO_2 to +1.29 in $VO_2(Ar)_2$ and to +1.18 in $VO_2(Xe)_2$, while the coordinated Ar and Xe atoms in $VO_2(Ar)_2$ and $VO_2(Xe)_2$ exhibit positive charges of +0.07 and +0.13, respectively.

$VO_4(Ng)$ (Ng = Ar, Xe). The 1121.9-, 975.3-, 974.1-, and 555.6-cm^{-1} absorptions increased on annealing at the expense of the $VO_2(Ar)_2$ absorptions. These bands were attributed initially to the O−O stretching, symmetric and antisymmetric VO_2 stretching, and $V{-}O_2$ stretching modes of VO_4 with the $OOVO_2$ (C_s) structure[13] but have been reassigned later to VO_4 with the $(O_2)VO_2$ (C_{2v}) structure.[34] The present experimental and theoretical results indicate that these absorptions should be

TABLE 2: Calculated Vibrational Frequencies (cm^{-1}) and Intensities (km/mol) for the Product Molecules at the B3LYP Level of Theory

molecule	frequency (intensity, mode)
VO_2 ($^2A_1$)	1026.6(34, a_1), 996.2(426, b_2), 262.1(4, a_1)
$VO_2(Ar)_2$ ($^2A_1$)	1013.9(43, a_1), 994.6(440, b_2), 312.8(26, a_1), 145.3(43, b_1), 114.6(0, a_1), 76.2(5, b_1), 61.5(26, b_1), 59.4(0, a_2), 42.9 (1, a_1)
$VO_2(Ar)(Xe)$ (^2A)	1008.4(52, a), 989.0(404, a), 313.4(21, a), 146.7(52, a), 103.0(0, a),74.5(3, a), 65.6(0, a), 64.6(20, a), 39.2(1, a)
$VO_2(Xe)_2$ ($^2A_1$)	1004.2(58, a_1), 985.5(370, b_2), 315.9(17, a_1), 149.0(55, b_1), 92.4(1, a_1) 75.6(2, b_2), 65.4(0, a_2), 62.5(19, b_1), 30.0(1, a_1)
VO_4 ($^2A_2$)	1198.9(62, a_1), 1077.0(114, a_1), 1073.4(326, b_1), 541.5(25, a_1), 522.2(8, b_2), 334.5(1, a_1), 221.7(0, a_2), 182.9(5, b_1), 134.3(78, b_2)
$VO_4(Ar)$ ($^2A''$)	1208.3(59, a), 1065.1(104.4, a), 1059.1(302, a), 542.0(31, a), 497.8(7, a), 331.0(4, a), 216.5(0, a), 185.6(3, a), 172.6(73, a), 100.2(9, a), 91.9(0, a), 85.6(0, a)
$VO_4(Xe)$ ($^2A''$)	1210.2(56, a), 1059.1(95 a), 1050.4(273, a), 540.4(36, a), 487.2(6, a), 329.3(7, a), 214.2(1, a), 197.5(81, a), 184.1(2, a), 94.8(0, a), 92.3(0, a), 81.0(1, a)
VO_6 (^4A)	1631.4(5, a), 1209.9(65, a), 1058.8(98, a), 1047.6(298, a), 541.2(31, a), 494.5(6, a), 330.0(4.5, a), 220.0(3, a), 217.7(0, a), 202.5(61, a), 188.6(3, a), 138.6(4, a), 136.7(0, a), 84.8(1, a), 39.8(0, a)

TABLE 3: Total V−Ng Binding Energies (kcal/mol) for the $VO_2(Ar)_{2-x}(Xe)_x$ ($x = 0, 1, 2$) and $VO_4(Ng)$ (Ng =Ar or Xe) Complexes Calculated at Various Levels of Theory

	$VO_2(Ar)_2$	$VO_2(Ar)(Xe)$	$VO_2(Xe)_2$	$VO_4(Ar)$	$VO_4(Xe)$	VO_6[a]
B3LYP	6.3	9.6	12.7	0.8	3.8	4.5
MP2	6.7	8.2	9.1	3.3	4.1	2.7
CCSD(T)//B3LYP	12.8	15.5	18.2	5.0	7.3	8.3

[a] The binding energies with respect to VO_4 ($^2A_2$) + O_2 ($^3\Sigma_g^-$).

TABLE 4: Calculated Natural Atomic Charges at the B3LYP Level of Theory

	V_1	$O_{2,3}$	O_3	O_4	Ar	Xe
VO_2	1.36	−0.68				
$VO_2(Ar)_2$	1.29	−0.72			0.07	
$VO_2(Ar)(Xe)$	1.24	−0.72			0.07	0.13
$VO_2(Xe)_2$	1.18	−0.72				0.13
VO_4	1.44	−0.52	−0.20	−0.20		
$VO_4(Ar)$	1.34	−0.51	−0.17	−0.22	0.08	
$VO_4(Xe)$	1.25	−0.51	−0.16	−0.22		0.16

reassigned to the $VO_4(Ar)$ complex. As shown in Figure 2, new absorptions at 1123.8, 970.9, and 968.4 cm^{-1} were produced when xenon was doped into the argon matrix, and these new absorptions increased on annealing after the 1121.9-, 975.3-, and 974.1-cm^{-1} absorptions. The 970.9- and 968.4-cm^{-1} bands shifted to 927.6 and 931.3 cm^{-1} with the $^{18}O_2$ sample and gave the $^{16}O/^{18}O$ isotopic frequency ratios of 1.0467 and 1.0398, respectively. These isotopic frequency ratios are about the same as those of the symmetric and antisymmetric VO_2 stretching vibrations of VO_2. The 1123.8-cm^{-1} band shifted to 1060.9 cm^{-1}. The $^{16}O/^{18}O$ isotopic frequency ratio of 1.0593 is indicative of an O−O stretching vibration. As shown in Figure 4, the 1123.8-cm^{-1} band split into a quartet with two intermediate absorptions at 1092.6 and 1090.1 cm^{-1} when a mixed 0.4% $^{16}O_2$ + 0.8% $^{16}O^{18}O$ + 0.4% $^{18}O_2$ sample was used. Similar quartet with intermediate absorptions at 1090.6 and 1088.3 cm^{-1} was also observed for the 1121.9-cm^{-1} band. The quartet structure observed in the mixed experiment indicates that the two O atoms in the O−O stretching mode are slightly inequivalent. The above-mentioned experimental observations suggest that the VO_4 molecule is coordinated by one noble gas atom in solid argon matrix. The 1121.9-, 975.3-, 974.1-, and 555.6-cm^{-1} absorptions are due to the $VO_4(Ar)$ complex isolated in solid argon, and the 1123.8-, 970.9-, and 968.4-cm^{-1} absorptions are assigned to the $VO_4(Xe)$ complex isolated in solid argon. The $V-O_2$ stretching mode of the $VO_4(Xe)$ complex is absorbed at the same position (555.6 cm^{-1}) as that of $VO_4(Ar)$.

Theoretical calculations support the above assignment. The VO_4 molecule was predicted to have a $^2A_2$ ground state with C_{2v} symmetry, in agreement with the previous reports.[9,34] The C_{2v} structure has two equivalent O atoms in the coordinated O_2 subunit and should split into a triplet for the O−O stretching mode in the mixed $^{16}O_2$ + $^{16}O^{18}O$ + $^{18}O_2$ experiment. This suggests that the observed absorptions at 1121.9, 975.3, 974.1, and 555.6 cm^{-1} in solid argon are not due to the isolated VO_4 molecule. Our theoretical calculations indicated that VO_4 could coordinate one argon atom in forming the $VO_4(Ar)$ complex. As shown in Figure 5, the $VO_4(Ar)$ complex has a $^2A''$ ground state with C_s symmetry. The Ar atom and the coordinated O_2 subunits are in the same plane that is perpendicular to the VO_2 plane. The O−O stretching, symmetric and antisymmetric VO_2 stretching, and the $V-O_2$ stretching modes of the $VO_4(Ar)$ complex were predicted to be 1208.2, 1065.4, 1059.2, and 541.7 cm^{-1}, respectively, in good agreement with the observed values. Since the two O atoms in the coordinated O_2 subunit are slightly inequivalent (V−O bond lengths of 1.958 and 2.007 Å, respectively, at the B3LYP level), a quartet with two intermediates should be observed for the O−O stretching mode in the mixed $^{16}O_2$ + $^{16}O^{18}O$ + $^{18}O_2$ spectrum, which is consistent with the experimental observations. When the Ar atom in $VO_4(Ar)$ was replaced by Xe, the above-mentioned vibrational modes were predicted to be 1210.3, 1059.0, 1050.2, and 539.1 cm^{-1}, respectively. The O−O stretching mode blue-shifted by 2.1 cm^{-1}, whereas the VO_2 stretching modes red-shifted by 6.4 and 9.0 cm^{-1} with respect to those of the $VO_4(Ar)$ complex, which are also in reasonable agreement with the experimentally determined shifts of 1.9, −4.4, and −5.7 cm^{-1}.

VO_6. The absorptions at 967.6 and 1127.2 cm^{-1} were observed in the experiments without Xe doping. These absorptions were assigned previously to VO_4 at different trapping sites in solid argon.[13] As can be seen in Figure 1, these two absorptions increased markedly on higher temperature annealing after the $VO_4(Ar)$ absorptions. We suggest that these bands are due to the VO_6 complex. Theoretical calculations predicted that VO_6 has a $^4A'$ ground state with C_s symmetry (Figure 5). The VO_6 structure can be regarded as an $(O_2)VO_2-OO$ complex with the Ar atom of $VO_4(Ar)$ being replaced by an O_2 unit. The V−OO bond length was predicted to be quite long (2.252 Å with B3LYP).

The V−Ng binding energies for the above-characterized complexes calculated at various levels of theory are listed in Table 3. The values calculated at the B3LYP level are smaller than those calculated at the CCSD(T) levels of theory because of the lack of proper treatment for dispersive interactions with B3LYP.[35] The binding energies per Ng for $VO_2(Ar)_2$ and $VO_2(Xe)_2$ are comparable with those previously reported transition metal−noble gas complexes[19−23,36,37] but are slightly larger than those of the $VO_4(Ar)$ and $VO_4(Xe)$ complexes. The predicted binding energies for the Xe complexes are larger than those for the Ar complexes, suggesting that xenon atoms can readily replace argon atoms in the coordination sphere of the VO_2 and VO_4 molecules, as experimentally observed. The binding energy of VO_6 with respect to $VO_4 + O_2$ is about the same as that of $VO_4(Xe)$ but is larger than that of $VO_4(Ar)$. Hence, the O_2 molecule can readily replace Ar atom of $VO_4(Ar)$ to form VO_6 in the experiments without Xe doping. In the Xe doping experiments, the VO_6 complex absorptions are barely observed, which suggests that the Xe atom is given preference over the O_2 molecule to replace the Ar atom of $VO_4(Ar)$.

Conclusions

The combination of matrix isolation infrared spectroscopic and quantum chemical calculation results provide strong evidence that vanadium dioxide and tetraoxide molecules, VO_2 and VO_4, coordinate noble gas atoms in forming noble gas complexes in solid noble gas matrixes. On the basis of the experiments using mixtures of argon doped with xenon, the number of noble gas atoms that bind intimately to the VO_2 and VO_4 molecules was determined. The results showed that VO_2 coordinates two Ar or Xe atoms and that VO_4 coordinates one Ar or Xe atom in solid noble gas matrixes. Hence, the VO_2 and VO_4 molecules trapped in solid argon matrix should be regarded as the $VO_2(Ar)_2$ and $VO_4(Ar)$ complexes. The assignment of a VO_6 complex is also suggested and its structure was theoretically predicted. The V−Ng binding energies of the characterized complexes were estimated at various levels of theory.

Acknowledgment. We gratefully acknowledge finical support from National Natural Science Foundation of China (Grant No. 20433080).

References and Notes

(1) Merer, A. J.; Huang, G.; Cheung, A. S. C.; Taylor, A. W. *J. Mol. Spectrosc.* **1987**, *125*, 465. Huang, G.; Merer, A. J.; Clouthier, D. J. *J. Mol. Spectrosc.* **1992**, *153*, 32. Adam, A. G.; Barnes, M.; Berno, B.; Bower, R. D.; Merer, A. J. *J. Mol. Spectrosc.* **1995**, *170*, 94. Ram, R. S.; Bernath, P. F.; Davis, S. P.; Merer, A. J. *J. Mol. Spectrosc.* **2002**, *211*, 279.

(2) Karlsson, L.; Lindgren, B.; Lundevall, C.; Sassenberg, U. *J. Mol. Spectrosc.* **1997**, *181*, 274.

(3) Maitre, P.; Bauschlicher, C. W., Jr. *Theor. Chim. Acta* **1985**, *90*, 189. Langhoff, S. R.; Bauschlicher, C. W., Jr. *J. Chem. Phys.* **1986**, *85*, 5936. Gutsev, G. L.; Andrews, L.; Bauschlicher, C. W., Jr. *Theor. Chem. Acc.* **2003**, *109*, 298.

(4) Dyke, J. M.; Gravenor, B. W. J.; Hastings, M. P.; Morris, A. *J. Phys. Chem.* **1985**, *89*, 4613.

(5) Carter, E. A.; Goddard, W. A. III. *J. Phys. Chem.* **1988**, *92*, 2109.

(6) Dolg, M.; Wedig, U.; Stoll, H.; Preuss, H. *J. Chem. Phys.* **1987**, *86*, 2123.

(7) Bakalbassis, E. G.; Stiakaki, M. D.; Tsipis, A. C.; Tsipis, C. A. *Chem. Phys.* **1996**, *205*, 389.

(8) Pykavy, M.; Wullen, V. C. *J. Phys. Chem. A* **2003**, *107*, 5566.

(9) Wu, H. B.; Wang, L. S. *J. Chem. Phys.* **1998**, *108*, 5310.

(10) Matsuda, Y.; Bernstein, E. R. *J. Phys. Chem. A* **2005**, *109*, 3803.

(11) Almond, M. J.; Atkins, R. W. *J. Chem. Soc., Dalton Trans.* **1994**, 835.

(12) Knight, L. B. Jr.; Babb, R.; Ray, M.; Banisaukas, T. J. III; Russon, L.; Dailey, R. S.; Davidson, E. R. *J. Chem. Phys.* **1996**, *105*, 10237.

(13) Chertihin, G. V.; Bare, W. D.; Andrews, L. *J. Phys. Chem. A* **1997**, *101*, 5090.

(14) Calatayud, M.; Silvi, B.; Andres, J.; Beltran, A. *Chem. Phys. Lett.* **2001**, *336*, 493.

(15) Gutsev, G. L.; Rao, B. K.; Jena, P. *J. Phys. Chem. A* **2000**, *104*, 11961.

(16) Schroder, D.; Schwarz, H.; Shaik, S. *Struct. Bonding* **2000**, *97*, 91.

(17) Jacox, M. E. *Chem. Soc. Rev.* **2002**, *31*, 108. Jacox, M. E. *Chem. Phys.* **1994**, *189*, 149.

(18) Li, J.; Bursten, B. E.; Liang, B.; Andrews, L. *Science* **2002**, *295*, 2242.

(19) Andrews, L.; Liang, B. Y.; Li, J.; Bursten, B. E. *J. Am. Chem. Soc.* **2003**, *125*, 3126. Andrews, L.; Liang, B. Y.; Li, J.; Bursten, B. E. *Angew. Chem., Int. Ed.* **2000**, *39*, 4565.

(20) Li, J.; Bursten, B. E.; Andrews, L.; Marsden, C. J. *J. Am. Chem. Soc.* **2004**, *126*, 3424.

(21) Wang, X. F.; Andrews, L.; Li, J.; Bursten, B. E. *Angew. Chem., Int. Ed.* **2004**, *43*, 2554.

(22) Zhao, Y. Y.; Wang, G. J.; Chen, M. H.; Zhou, M. F. *J. Phys. Chem. A* **2005**, *109*, 6621.

(23) Zhao, Y. Y.; Gong, Y.; Chen, M. H.; Ding, C. F.; Zhou, M. F. *J. Phys. Chem. A* **2005**, *109*, 11765.

(24) Chen, M. H.; Wang, X. F.; Zhang, L. N.; Yu, M.; Qin, Q. Z. *Chem. Phys.* **1999**, *242*, 81. Zhou, M. F.; Andrews, L. Bauschlicher, C W., Jr. *Chem. Rev.* **2001**, *101*, 1931.

(25) Frisch, M. J.; Trucks, G. W.; Schlegel, H. B.; Scuseria, G. E.; Robb, M. A.; Cheeseman, J. R.; Montgomery, J. A., Jr.; Vreven, T.; Kudin, K. N.; Burant, J. C.; Millam, J. M.; Iyengar, S. S.; Tomasi, J.; Barone, V.; Mennucci, B.; Cossi, M.; Scalmani, G.; Rega, N.; Petersson, G. A.; Nakatsuji, H.; Hada, M.; Ehara, M.; Toyota, K.; Fukuda, R.; Hasegawa, J.; Ishida, M.; Nakajima, T.; Honda, Y.; Kitao, O.; Nakai, H.; Klene, M.; Li, X.; Knox, J. E.; Hratchian, H. P.; Cross, J. B.; Adamo, C.; Jaramillo, J.; Gomperts, R.; Stratmann, R. E.; Yazyev, O.; Austin, A. J.; Cammi, R.; Pomelli, C.; Ochterski, J. W.; Ayala, P. Y.; Morokuma, K.; Voth, G. A.; Salvador, P.; Dannenberg, J. J.; Zakrzewski, V. G.; Dapprich, S.; Daniels, A. D.; Strain, M. C.; Farkas, O.; Malick, D. K.; Rabuck, A. D.; Raghavachari, K.; Foresman, J. B.; Ortiz, J. V.; Cui, Q.; Baboul, A. G.; Clifford, S.; Cioslowski, J.; Stefanov, B. B.; Liu, G.; Liashenko, A.; Piskorz, P.; Komaromi, I.; Martin, R. L.; Fox, D. J.; Keith, T.; Al-Laham, M. A.; Peng, C. Y.; Nanayakkara, A.; Challacombe, M.; Gill, P. M. W.; Johnson, B.; Chen, W.; Wong, M. W.; Gonzalez, C.; Pople, J. A. *Gaussian 03*, revision B.05; Gaussian, Inc.: Pittsburgh, PA, 2003.

(26) Becke, A. D. *J. Chem. Phys.* **1993**, *98*, 5648.

(27) Lee, C.; Yang, E.; Parr, R. G. *Phys. Rev. B* **1988**, *37*, 785.

(28) Moller, C.; Plesset, M. S. *Phys. Rev. B* **1984**, *46*, 618.

(29) McLean, A. D.; Chandler, G. S. *J. Chem. Phys.* **1980**, *72*, 5639. Krishnan, R.; Binkley, J. S.; Seeger, R.; Pople, J. A. *J. Chem. Phys.***1980**, *72*, 650.

(30) Andrae, D.; Haussermann, U.; Dolg, M.; Stoll, H.; Preuss, H. *Theor. Chim. Acta.* **1990**, *77*, 123.

(31) Pople, J. A.; Gordon, M. H.; Raghavachari, K. *J. Chem. Phys.* **1987**, *87*, 5968.

(32) Andrews, L.; Ault, B. S.; Grzybowski, J. M.; Allen, R. O. *J. Chem. Phys.* **1975**, *62*, 2461. Chertihin, G. V.; Andrews, L. *J. Chem. Phys.* **1998**, *108*, 6404. Chertihin, G. V.; Saffel, W.; Yustein, J. T.; Andrews, L.; Neurock, M. Ricca, A.; Bauschlicher, C. W. *J. Phys. Chem.* **1996**, *100*, 5261.

(33) Thompson, W. E.; Jacox, M. E. *J. Chem. Phys.* **1989**, *91*, 3826.

(34) Zhou, M. F.; Andrews, L. *J. Phys. Chem. A* **1998**, *102*, 8251.

(35) Ono, Y.; Taketsugu, T. *Chem Phys Lett* **2004**, *385*, 85.

(36) Wells, J. R.; Weitz, E. *J. Am. Chem. Soc.* **1992**, *114*, 2783.

(37) Sun, X. Z.; George, M. W.; Kazarian, S. G.; Nikiforov, S. M.; Poliakoff, M. *J. Am. Chem. Soc.* **1996**, *118*, 10525.